Light Scattering and Viscoelasticity in Aqueous Mixtures of Oppositely Charged and Hydrophobically Modified Polyelectrolytes

Marina Tsianou,[†] Anna-Lena Kjøniksen,[‡] Krister Thuresson,[†] and Bo Nyström*[,‡]

Physical Chemistry 1, Chemical Centre, University of Lund, P.O. Box 124, S-221 00 Lund, Sweden, and Department of Chemistry, University of Oslo, P.O. Box 1033, Blindern, N-0315, Oslo, Norway

Received October 16, 1998; Revised Manuscript Received March 2, 1999

ABSTRACT: Rheological and intensity (ILS) and dynamic light scattering (DLS) experiments were performed on semidilute aqueous mixtures of various compositions of oppositely charged and hydrophobically modified polyelectrolytes. The associative phase separation usually observed when mixing oppositely charged polyelectrolytes is restricted to a fairly narrow mixing region when the polymers are hydrophobically modified. Measurements were carried out at mixing ratios both before and after this two-phase area. The rheological properties in the vicinity of the two-phase region show that the elastic response dominates even at fairly low frequencies, indicating the existence of strong intermolecular interactions. The time correlation data obtained from the DLS experiments revealed the existence of two relaxation modes, one single exponential at short times followed by a stretched exponential at longer times. The fast mode is always diffusive, and the extracted hydrodynamic correlation length as well as the static one from ILS increases toward phase separation of the mixture. The slow relaxation time reveals that the dynamics slowed down in the vicinity of phase separation, and the angular dependence of the slow mode is stronger than that of the fast mode and increases gradually as the two-phase region is approached. These features that are attributed to enhanced hydrophobic associations can be rationalized in the framework of the coupling model of Ngai. The fractal dimension, determined from ILS, drops toward phase separation, and this trend suggests a more "open" network structure at this stage.

Introduction

The interactions between ionic polymers and surfactants of opposite charge have been well characterized over the past few decades.[1−7] The mixing of an aqueous solution of an ionic polymer with an oppositely charged surfactant generally results in an associative phase separation. This phenomenon is well documented,[8] and in this process a concentrated phase is formed that is enriched in both the charged polymer and the surfactant. The association between surfactants and polyelectrolytes of opposite charge is primarily electrostatic in nature and is reminiscent[2] of the phase separation behavior in mixtures of two oppositely charged polymers. One of the most intriguing challenges of this type of system is the interaction between cationic and anionic macromolecules in aqueous solutions, leading to the formation of polyelectrolyte complexes.[9−19] Although investigations of polyelectrolyte complexes have a quite lengthy history, there have been relatively few attempts to examine and interpret the changes in the structural and dynamical properties of mixtures of oppositely charged polyelectrolytes.

Recently, the effect of hydrophobic modification on phase behavior in aqueous mixtures of oppositely charged polyelectrolytes was studied.[17] It was found that mixtures of hydrophobically unmodified polyelectrolytes exhibit associative phase separation over a large part of the mixing range. The driving force in this process is the entropy of counterion distribution.[16] However, if both the oppositely charged polyelectrolytes are hydrophobically modified, an additional effect comes into play, namely the tendency to form mixed aggregates; as a result, the associative phase separation behavior is effectively prevented in a large mixing region, and there is only a narrow two-phase domain. Rheological measurements[17] have revealed interesting features of this type of system on addition of one polyelectrolyte to the other, especially when the associative phase separation region is approached. The observed viscosity enhancement of this mixture of one cationic and one anionic hydrophobically modified polyelectrolyte was attributed to a formation of mixed aggregates consisting of hydrophobic tails from polyelectrolytes bearing charges of opposite sign. In light of this, we also expect profound changes of the structural and dynamical properties of these systems as the two-phase region is approached.

In this paper we report results from intensity light scattering (ILS), dynamic light scattering (DLS), and rheological measurements of semidilute mixtures of two oppositely charged and hydrophobically modified polyelectrolytes. The aim of this work is to gain a deeper insight into how the composition affects the structural characteristics and the dynamics of this type of mixture.

Experimental Section

Materials. The characteristic data of the hydrophobically modified cationic polymer QUATRISOFT LM200 (HM-P^+) and of the hydrophobically modified polyacrylate (HM-P^-), which was chosen as the negatively charged polyelectrolyte, are collected in Table 1. The cationic polymer (HM-P^+), which is a *N*,*N*-dimethyl-*N*-dodecylammonium derivative of hydroxyethylcellulose (a representative structure of the polymer is given in Figure 1) with a molecular weight of approximately 100 000,[20] was manufactured by Union Carbide Chemicals and Plastics Company, Inc. The charges are located at the hydrophobic tails (see the schematic illustration in Figure 1), giving a structure of the hydrophobic side chain resembling that of a cationic surfactant. LM200 is a weakly charged hydrophobically modified cationic polyelectrolyte. This polymer was used in its chloride salt form. The degree of hydrophobic substitution

[†] University of Lund.
[‡] University of Oslo.
* Corresponding author.

10.1021/ma981619c CCC: $18.00
Published on Web 04/09/1999

Table 1. Characteristic Data for the HM-P$^+$ and HM-P$^-$ Polymers

	HM-P$^+$	HM-P$^-$
molecular weight	100 000	200 000
charge	positive	negative
concentration of charges in a 1 wt % aqueous solution (*m*m)	2	99
mean contour length between charges (Å)	100	2.5
hydrophobic modification degree (mol %)	5.4	3
mean contour length between hydrophobic tails (Å)	100	84

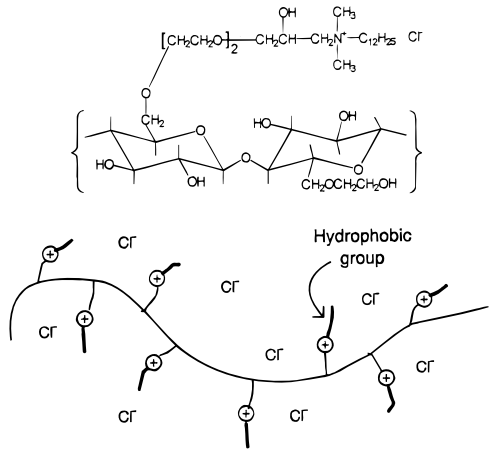

Figure 1. Idealized structure and a schematic illustration of the cationic hydrophobically modified polymer, denoted HM-P$^+$.

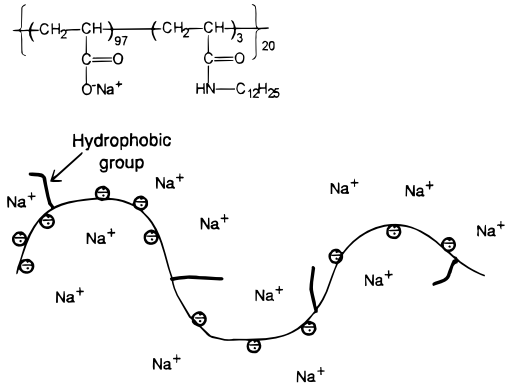

Figure 2. A representative structure and a schematic illustration of the anionic hydrophobically modified polyacrylate, denoted HM-P$^-$. We should note that this rough outline does not give the exact depiction of the ratio of hydrophobic tails to charges.

has been obtained by nitrogen analysis of the dry polymer and found to be 2.0×10^{-4} mol of hydrophobic chains per gram of polymer, which roughly corresponds to 5.4 side chains per 100 sugar residues. The hydroxyethyl substitution of LM200 is not known but can possibly vary from $MS_{EO} = 0$ to $MS_{EO} = 3.3$.[4,17] Low molecular weight impurities were removed by dialysis against Millipore water in a Filtron Ultrasette device, and the polymer was recovered by freeze-drying.

The anionic hydrophobically modified polyacrylate (HM-P$^-$) has a substitution degree of 3 mol % dodecyl chains grafted to the polymer backbone and a molecular weight of approximately 200 000 in the sodium form. The negative charges are located along the polymer backbone, and a typical structure of the polymer is given in Figure 2. The HM-P$^-$ sample was obtained as a kind gift from Dr. Iliopoulos, Université Pierre et Marie Curie, Paris, and was used as received. The experimental details of the hydrophobic modification have been described elsewhere.[21]

Sample Preparation and Phase Behavior. All samples were individually prepared by mixing stock solutions of the respective polymers at different ratios. The solutions of the single polyelectrolyte components and the mixtures were prepared at a constant total concentration of 1 wt %. The pH of 1 wt % HM-P$^-$ solution utilized in this study is about 10. Addition of HM-P$^+$ to HM-P$^-$ does not introduce any components that will influence the pH and lower it to the extent that HM-P$^-$ is partially charged. All water used was of MilliQ quality. The samples were carefully mixed by stirring, or for viscous samples by centrifugation in alternating directions, at room temperature for several days. After equilibration, the samples were centrifuged for at least 24 h, and the phase behavior was determined by visual inspection. The phase boundaries of the two-phase region for the system under investigation have been previously determined by Thuresson et al.[17] The two-phase region extends from about 2 to 21 wt % HM-P$^-$. The one-phase samples are homogeneous and optically clear, often highly viscous gels. Most of the two-phase samples display two well-separated phases. The top phases are transparent and of low viscosity, while the bottom ones have the appearance of gellike white precipitate. Opaque samples showing no macroscopic phase separation (commonly close to the phase boundaries) are considered to be biphasic. No extra salt has been added in the system. It should be mentioned here that the final mixtures of the two polyelectrolytes have not been dialyzed; thus, the samples contain small amounts of salt due to the association of the two polyions and the release of counterions. The exact amount of screening salt will therefore vary with the mixture composition. The rheological and light scattering measurements in this investigation have been performed to samples well within the one-phase region. The samples prepared for the light scattering experiments were filtered in an atmosphere of filtered air through 0.8 μm filters (Micro Filtration Systems) directly into precleaned 10 mm NMR tubes (Wilmad Glass Co.) of highest quality. All measurements were carried out at 25 °C.

Oscillatory Experiments. The oscillatory shear measurements were conducted on a CarriMed CSL 100 constant stress rheometer, equipped with an automatic gap setting. Depending on the viscosity of the sample, 1° acrylic cone and plate geometry with a diameter of 4 or 6 cm, respectively, was used. In the present study the results from the oscillatory sweep measurements in the approximate frequency range 0.01−20 Hz are reported. The values of the stress amplitude were checked in order to ensure that all measurements were performed within the linear viscoelastic region, where the dynamic storage modulus (G') and loss modulus (G'') are independent of the applied stress. The temperature in the sample chamber was controlled to within ±0.1 °C with the aid of a Peltier plate.

Light Scattering Experiments. In light scattering experiments we probe on a length scale of q^{-1}, where q is the wave vector defined as $q = 4\pi n \sin(\theta/2)/\lambda$. Here λ is the wavelength of the incident light in a vacuum, θ is the scattering angle, and n is the refractive index of the medium. The value of n was determined at $\lambda = 488$ nm for each composition with an Abbé refractometer.

The light scattering experiments were conducted on a standard laboratory built light scattering spectrometer capable of doing both absolute integrated scattering intensity and photon correlation measurements at different scattering angles. The intensity light scattering (ILS) measurements were carried out using ALV (Langen-Germany) light scattering electronics in combination with the on-line program ODIL. A Spectra Physics model 2020 argon ion laser operating at a wavelength of 488 nm was used. The light was vertically polarized, and the intensity of the output beam was adjusted with the aid of high-quality neutral density filters (Melles Griot) of various transmittances depending upon the intensity of the scattered light from the samples. To ensure a vv configuration, polarizers were placed both in front and behind the cell. The sample cell was held in a thermostat block filled with refractive index matching dibutyl phthalate, and the temperature was controlled to within ±0.05 °C.

In the present experimental configuration a detection geometry was utilized where a vertical slit, instead of the usual pinhole, was placed in front of the photomultiplier tube. With this arrangement, the absolute quantity $R_{vv}(q)$, which is the excess Rayleigh ratio with vertically polarized incident and scattered beams, can be determined from the relation $R_{vv}(q) = hI^*(q)$, where $I^*(q)$ is the excess scattered intensity and $h = R_{vv,benzene}n_{solv}/(I^*_{benzene}n_{benzene})$. A value of $R_{vv}(90°) = 3.14 \times 10^{-5}$ cm^{-1} reported[22] for benzene at 25 °C and 488 nm was used in this work. The optical constant K (cm^3 mol g^{-2}) was calculated from $K = (4\pi^2n^2/N_A\lambda^4)(\partial n/\partial c)^2$, where N_A is Avogrado's constant, $\partial n/\partial c$ is the refractive index increment, and c is the mass/volume concentration. The values of the refractive index increment for the different mixture compositions were determined with a Brice-Phoenix differential refractometer (model BP-2000-V). The reduced scattered intensity, $Kc/R_{vv}(q)$ was calculated from a Guinier plot[23] of $\ln(Kc/R_{vv}(q))$ versus q^2.

In the DLS experiments, the full homodyne intensity autocorrelation function was determined with an ALV-5000 multiple-τ-digital correlator. The correlation functions were recorded in the real time "multiple-τ" mode of the correlator, in which 256 time channels are logarithmically spaced over an interval ranging from 0.2 μs to almost an hour.

The Siegert relation[24] relates the normalized intensity autocorrelation function $g^{(2)}(q,t)$ to the normalized electric field autocorrelation function $g^{(1)}(q,t)$, assuming the scattered field has Gaussian statistics.

$$g^{(2)}(q,t) = 1 + B|g^{(1)}(q,t)|^2 \quad (1)$$

where B (≤ 1) is an instrumental parameter.

In the case of semidilute associating polymer systems, one usually observes[25−31] a bimodal time autocorrelation function consisting of one single-exponential decay associated with cooperative diffusion ($\tau_f^{-1} = D_cq^2$, where τ_f is the "fast" relaxation time and D_c is the cooperative diffusion coefficient) and a group of relaxation modes characterizing disengagement relaxation of individual chains[27,32] or cluster relaxation.[33] Since time correlation functions of the concentration fluctuations at long wavelengths in the semidilute regime were recorded, the fast mode was always observed to be diffusive (q^2 dependent). We have found that the slow relaxation process can be described by a stretched exponential, and this mode exhibits a more complex q dependence that will be discussed below. Thus, in this work, as well in other DLS investigations[28−31] on complex polymer systems, all the correlation data were analyzed by using the following heuristic expression

$$g^{(1)}(t) = A_f \exp(-t/\tau_f) + A_s \exp[-(t/\tau_{se})^{\beta}] \quad (2)$$

with $A_f + A_s = 1$. This relationship is found to capture the characteristic features of the present systems. The parameters A_f and A_s are the amplitudes for the fast and slow relaxation modes, respectively. The variable τ_{se} is some effective slow relaxation time, and the stretched exponent β ($0 < \beta \leq 1$) is an indication of the width of the distribution of relaxation times. The β variable has been interpreted[32] as a measure of inhomogeneity or disorder effects of the system, and the specific value of β depends on the topological dimension of the modeled cluster. As will be shown below, the value of β in this study depends strongly on the composition of the polyelectrolyte mixture. The mean slow relaxation time is given by

$$\tau_s \equiv \int_0^{\infty} \exp\left[-\left(\frac{t}{\tau_{se}}\right)^{\beta}\right] dt = \frac{\tau_{se}}{\beta}\Gamma\left(\frac{1}{\beta}\right) \quad (3)$$

where $\Gamma(\beta^{-1})$ is the gamma function of β^{-1}.

In the analysis of the correlation function data, a nonlinear fitting algorithm (a modified Levenberg−Marquardt method) was utilized to obtain best-fit values of the parameters A_f, τ_f, τ_{se}, and β appearing on the right-hand side of eq 2. A fit was considered satisfactory if there were no systematic deviations in the plot of the residuals of the fitted curve.

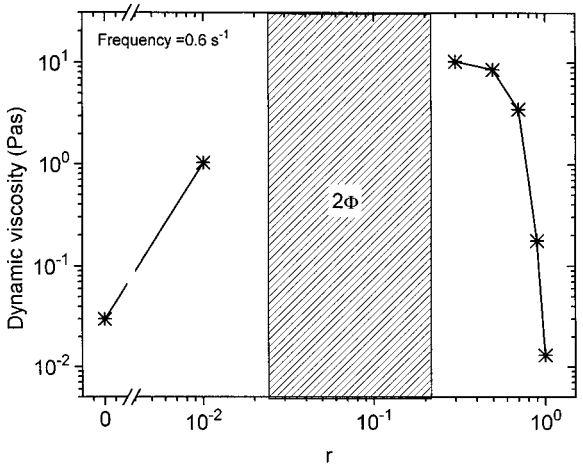

Figure 3. Dynamic viscosity at 0.6 Hz of mixtures of HM-P^+ and HM-P^- as a function of the mixture ratio r ($r = m_{HM-P^-}/(m_{HM-P^-} + m_{HM-P^+})$). The total polymer concentration is kept at 1 wt %.

Results and Discussion

Before we present and discuss the results, it may be instructive to give some basic aspects on this type of system. It is usually considered that polyelectrolyte complexes are formed by oppositely charged polyelectrolytes due to Coulomb forces. However, for a detailed description of the associative microphase separation in polyelectrolyte systems, we must consider the delicate interplay[16] between, at least, three main factors, namely non-Coulombic repulsion between dissimilar monomer units (or monomer−solvent repulsion) leading to immiscibility in the absence of charges, translational entropy of small counterions enhancing miscibility, and electrostatic interactions between charged microdomains. When both polyelectrolytes are hydrophobically modified, the interaction situation is strongly modulated by the attractive hydrophobic interactions, and there is an enhanced tendency of the system to form mixed aggregates. The conjecture[17] is that this behavior should give rise to a net charge of the macromolecular part of the concentrated phase and, hence, to an entropy loss in the counterion distribution on phase separation. To counteract the increase in free energy of the system, the concentrated phase swells, and the tendency of phase separation is reduced or completely eliminated, depending on the charge stoichiometry. The observed[17] reduction of the two-phase region in mixtures of HM-P^-/HM-P^+ as compared to that for the unmodified polymers can be rationalized in this framework.

Viscoelastic Properties. Figure 3 shows the dynamic viscosity η' at a low frequency of 0.6 Hz of mixtures of HM-P^+ and HM-P^-, at a total polymer concentration of 1 wt %, as a function of the mixture ratio $r = m_{HM-P^-}/(m_{HM-P^-} + m_{HM-P^+})$ (m denotes the mass of the considered component). We may note that the dynamic viscosity of a 1 wt % aqueous solution of pure HM-P^- ($r = 1$) is lower than the viscosity of 1 wt % aqueous solution of HM-P^+ ($r = 0$). This trend can probably be related to the different nature of the cellulosic polymers. When the negatively charged polyelectrolyte HM-P^- is added to a solution of HM-P^+, a marked rise of the viscosity is observed as the two-phase region is approached. The viscosity increase can prob-

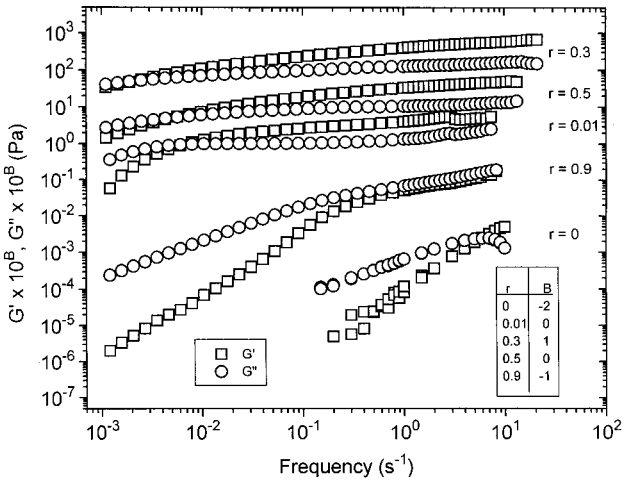

Figure 4. Frequency dependences of the storage modulus (G') and the loss modulus (G'') for mixtures of different composition at a total concentration of 1 wt %. The curves have been shifted vertically by a factor B of the value listed in the inset. The vertical trend of the data has not been changed by this action.

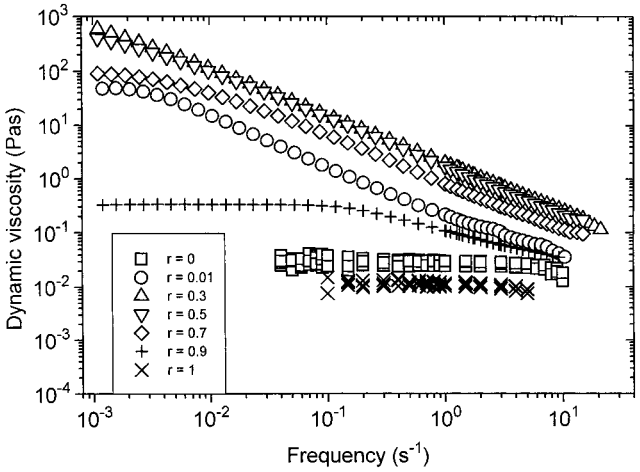

Figure 5. Effect of the frequency of oscillation on the dynamic viscosity of mixtures of various compositions at a total concentration of 1 wt %.

ably be attributed to a combined effect of electrostatic interactions and hydrophobic associations. When the amount of the HM-P$^-$ polymer in the mixture increases, the charges on HM-P$^+$ are screened, and this effect promotes clustering of the hydrophobic tails of the polymers. At higher concentrations of the anionic polymer (on the right-hand side of the two-phase domain), there is a balance between the electrostatic and the hydrophobic interactions. As a result of this process, the viscosity drops significantly as the weight fraction of HM-P$^-$ increases (see Figure 3).

In Figure 4, the dynamic storage and loss moduli of mixtures of HM-P$^+$ and HM-P$^-$ at a total polymer concentration of 1 wt % are plotted against frequency. The curves have been purposely shifted vertically by a factor B (see the inset in Figure 4) for easier comparison. For 1 wt % solutions of the pure components (the result for the HM-P$^+$ ($r = 0$) solution is shown), the systems tend to behave classically as a Newtonian liquid ($G' \sim \omega^2$ and $G'' \sim \omega^1$). The experimental scatter (at low frequencies) of the G' data at $r = 0$ is probably due to the weak elastic response at this system (low viscous solution). The general picture that emerges is that, at low or very low frequencies, we observe a viscous behavior with $G'' > G'$, while at higher frequencies, depending on the composition of the mixture, G' increases to cross G'', and above this frequency, G' exceeds G'', which suggests that the elastic response dominates. It is evident that the frequency of intersection is located at low frequencies (long times of intersection) for mixtures with values of r close to the two-phase region, while systems far removed from this domain exhibit high frequencies of intersection. These findings suggest that the networks formed in the vicinity of the two-phase region contain entangled or interconnected chains. Furthermore, these results may indicate the formation of large and more open network structures (see the discussion below).

Rheological data from polymer systems are frequently analyzed in the framework of the simplest model of a viscoelastic fluid, namely the Maxwell model. This simple model, consisting of an elastic component (spring) connected in series with a viscous component (dashpot), is used to describe the frequency dependencies of the dynamic moduli. However, neither a single Maxwell element nor a sum[34] of Maxwell elements could be used to properly describe the frequency dependencies of G' and G'' for the present mixtures of HM-P$^+$ and HM-P$^-$. These findings indicate that there is not a single relaxation time that controls the time scale, but a more complex picture, with a broad distribution of relaxation times, emerges. We may note that the failure of the Maxwell model to describe rheological data of complex polymer systems has also been reported[31,34] for aqueous solutions of a hydrophobically modified ethyl(hydroxyethyl)cellulose and its unmodified analogue in the presence of a surfactant.

The effect of the frequency of oscillation on the dynamic viscosity of 1 wt % solutions of the pure components and of mixtures of various compositions is given in Figure 5. The results indicate that the polyelectrolyte systems become more viscoelastic, i.e., displaying increased frequency dependence, typical of polymer network systems containing cross-linked or entangled chain networks, as the values of r approach the two-phase region. For solutions of the pure polymer components, η' is virtually independent of frequency, and the systems display rheological characteristics typical of unentangled polymer solutions. These results emphasize again the formation of a association network in the neighborhood of phase separation.

Dynamic Light Scattering. Figure 6 shows time correlation data at a scattering angle of 30° for mixtures of HM-P$^+$ and HM-P$^-$, together with the corresponding curves fitted with the aid of eq 2. The inset in Figure 6 shows semilogarithmic plots of $g^1(t)$ as a function of t^β for the compositions indicated. This type of plot yields straight lines for functions that can be represented by stretched exponentials. We observe that, within experimental error, the long-time behaviors of the correlation functions are well described by straight lines. An inspection of the correlation functions reveals that the long-time tail is shifted toward long times for mixtures with compositions that are located close to the two-phase region.

By using the model equation (see eqs 2 and 3), a number of characteristic parameters can be determined. Let us first discuss the fast relaxation time which yields the cooperative diffusion coefficient D_c from which the apparent hydrodynamic correlation length ξ_h can be estimated through the expression[35] $D_c \cong k_B T/6\pi\eta_0\xi_h$, where k_B is the Boltzmann constant, T is the absolute

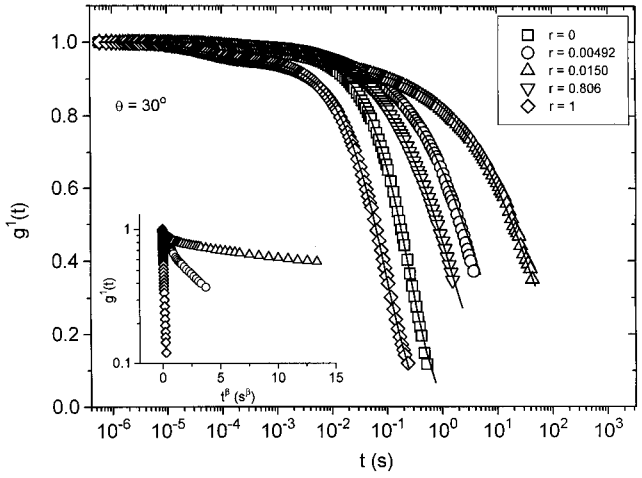

Figure 6. First-order electric field correlation function versus time (every third point is shown) for 1 wt % solutions of the mixture ratios and scattering angle indicated. The curves are fitted with the aid of eq 2. The inset plot demonstrates the stretched exponential character of the correlation functions at long time.

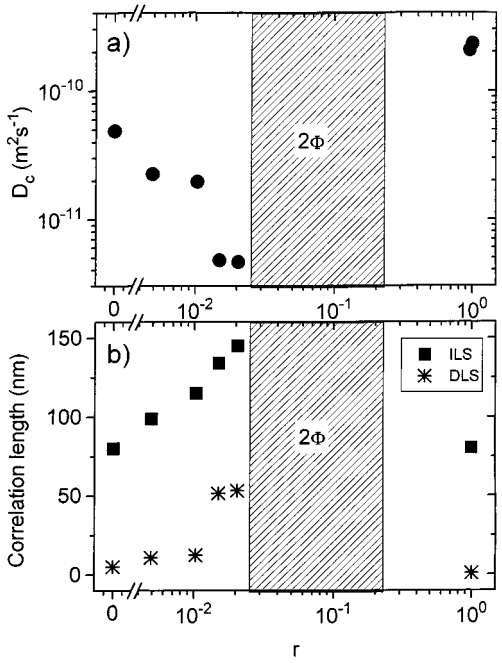

Figure 7. Effects of mixture ratio at a total polymer concentration of 1 wt % on the cooperative diffusion coefficient and the static and hydrodynamic correlation length.

temperature, and η_0 is the solvent viscosity. The effect of mixture composition on these quantities is illustrated in Figure 7 for solutions of a total polymer concentration of 1 wt %. The lack of data points on the right-hand side of the two-phase domain is due to problems with the separation of the different relaxation modes of the correlation function. At mixture ratios close to this region, the profile of the correlation function is complex, and we have not in an unambiguous way succeeded to separate the contributions from the two polymer components. At low or high ratios of r, one of the polymers dominates in the mixtures, and the relaxation process is practically governed by this component. In this case the fast and the slow relaxation modes are readily extracted from the decay of the correlation function. It is evident from the data in Figure 7 that D_c drops as the two-phase region is approached and rises (the right-hand side of the two-phase region) as the composition is changed toward the pure HM-P$^-$ component. This behavior may be rationalized in the following way. The diffusion process is governed by the interplay between hydrodynamic and thermodynamic properties through the relationship[35] $D \cong s\,\partial\Pi/\partial c$, where s (the hydrodynamic factor) is the sedimentation coefficient and $\partial\Pi/\partial c$ is the inverse osmotic compressibility. At a given concentration, the thermodynamic factor $\partial\Pi/\partial c$ is expected to play a dominating role in the diffusion behavior. Since this factor decreases when the thermodynamic conditions become poorer, we expect that D_c falls off as the two-phase region is approached.

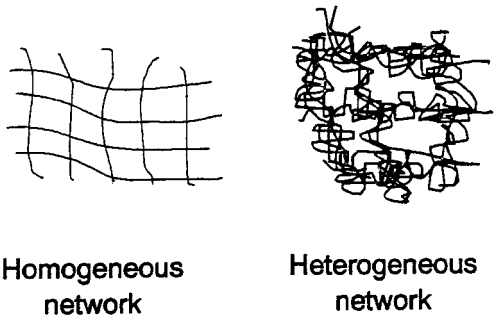

Figure 8. Illustration of the structural reorganization of the polymer network from homogeneous (pure polyelectrolytes) to heterogeneous as the two-phase region is approached. In the latter stage, bundles of polycation and polyanion chains are formed in the network, and the average spacings between bundles are larger than the average mesh size of the homogeneous network.

The effect of the mixture composition on the hydrodynamic correlation length is displayed in Figure 7. The values of the static correlation length ξ, obtained from the ILS measurements (see also the discussion below) by using eq 9, have also been included. Although the values of the static correlation length are much higher than the corresponding dynamic ones, calculated from the fast relaxation time of the correlation function, the general trend is the same. If the correlation length is visualized[35] as a measure of the average mesh size of the network, the observed rise of the correlation length as the two-phase region is approached may be associated with a combination of attractive Coulomb forces and hydrophobic associations at these conditions, giving rise to a heterogeneous network. The conjecture is that bundles of close-packed polycation and polyanion chains are formed (see Figure 8), and as a result, the effective mesh size of the network increases. In this context it is interesting to draw our attention to a recent diffusion study,[36] dealing with changes of the diffusion features in connection with formation of nonuniformities of networks undergoing sol−gel transitions. In the mentioned investigation, the diffusion behavior in gels and the corresponding solutions was analyzed, and it was found that nonuniformities in the network play an important role for the diffusion properties. Depending on the magnitude of these nonuniformities, the cooperative diffusion coefficient of the gel may be smaller than, equal to, or greater than the corresponding value of the solution. The model predicts a reduction of the diffusion coefficient for a system with increasing nonuniformity of the network. In light of this approach, the present results of D_c may suggest that the nonuniformities of the networks increase when the two-phase region is approached.

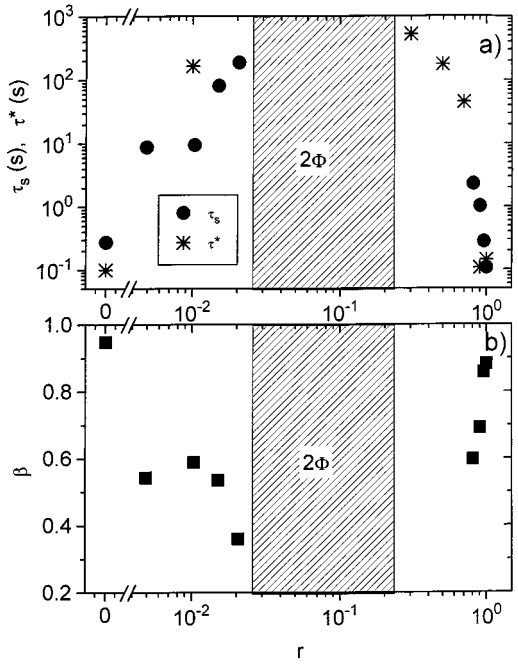

Figure 9. Effects of mixture ratio (total polymer concentration of 1 wt %) on the slow relaxation time τ_s and the time of intersection τ^* (a) and the stretched exponent β (b).

Figure 9 shows how the slow relaxation time τ_s is affected by the composition of the mixture. The rheological analogue, the time of intersection $\tau^* = 1/2\pi f^*$, corresponding to the frequency of intersection f^* where G' equals G'' (see Figure 4), is also displayed in Figure 9. Both quantities exhibit the same type of behavior, with strongly increasing values of the relaxation time as the two-phase domain is approached. The dynamical slowing down may be due to enhanced associations in the vicinity of the two-phase region. These results suggest that the relaxation processes operating in rheology and DLS are slow, and a picture emerges where groups of chains move together, leading to a distribution of relaxation times associated with the cluster size distribution.

In Figure 9b, the stretched exponent β is plotted as a function of the mixture ratio r. It is evident that the value of β drops strongly when the two-phase region is approached. There are theoretical models that can rationalize this type of behavior. Recently, Douglas and Hubbard[32] formulated a semiempirical approach to relaxation in condensed materials, which addresses material inhomogeneity through the parameter β. The value of β was interpreted as a measure of inhomogeneity or disorder effects of the system, and the specific value of β depends on the topological dimension of the modeled cluster. In view of this model, the observed drop of β suggests enhanced inhomogeneity effects of the mixture.

In the coupling model of Ngai,[33] the value of the stretch exponent β, or the value of the coupling parameter n ($\beta = 1 - n$) is a direct measure of the coupling strength of the relaxation mode to its complex environments. The coupling model[37−41] provides a general approach to the dynamics of constrained, interacting systems. In this framework, the system under consideration is said to be composed of "basic units", which interact nonlinearly and more or less strongly with each other. There exists a crossover time t_c, which separates short and long time regimes. At short times ($t \leq t_c$) the basic units relax independently, their temporal correlation function (an example is the field correlation function) having the general form

$$\phi(t) = \exp(-t/\tau_0) \qquad t < t_c \tag{4}$$

At longer times the correlation function is characterized by the slowed down stretched exponential function

$$\phi(t) = \exp[-(t/\tau^*_s)^{1-n}] \qquad t > t_c \tag{5}$$

where n depends on the intermolecular interaction and whose value lies within the range $0 \leq n < 1$. The basic features of this model suggest that n rises (or β decreases) as the strength of the interaction between the basic units is increased. The quantity τ_0 is a relaxation time characteristic of the unconstrained motions of the basic dynamic units, while τ^*_s describes the average relaxation time of the basic dynamic units at longer times, after cooperative constraint dynamics between the relaxing basic units has come into play. Continuity of the two processes of the correlation function at $t = t_c$ leads immediately to the important relationship

$$\tau^*_s = [t_c^{-n}\tau_0]^{1/(1-n)} \tag{6}$$

This equation links the effective relaxation time τ^*_s to the independent relaxation time τ_0 and the crossover time t_c.

In light of the coupling model, the observed effects of mixture composition on the stretched exponent β (Figure 9b) and on the slow relaxation time (Figure 9a) can be rationalized. As the two-phase region is approached, the intermolecular interactions are strengthened, and polymer clustering and thus "entanglement-like" response should be favored. As a result, the strength of interaction or coupling strength increases; that is, β drops which is in accord with the experimental observation for the present system. The coupling model further predicts (see eq 6) that the slow relaxation time should increase with decreasing β. This prediction is also consistent with the experimental finding (cf. Figure 9a).

The angular dependence of the correlation function, at different mixture ratios, is illustrated in the form of a reduced plot in Figure 10. The general trend is that correlation function data practically condense onto a single curve at short times, reflecting the diffusive character (q^2 dependent) of the fast mode. However, the long-time tails of the correlation functions are more or less separated, depending on the composition of the mixture, indicating a q dependence stronger than that for a diffusive process. This complex q dependence of the slow mode will be discussed below.

To quantitatively evaluate the q dependences of the relaxation times (τ_f and τ_s), plots of the inverse relaxation times as a function of q are depicted in Figure 11a. From the slopes of the straight lines, the numerical values of the scaling law exponents α_f and α_s are determined. The value of α_f is within error equal to 2 at all conditions, suggesting that the fast mode is diffusive. The value of α_s rises in the vicinity of the two-phase region (see Figure 11b), and a strong q dependence of the slow mode is revealed. The present experimental findings of the q dependences of the fast and the slow mode can be interpreted in the framework of the coupling model.

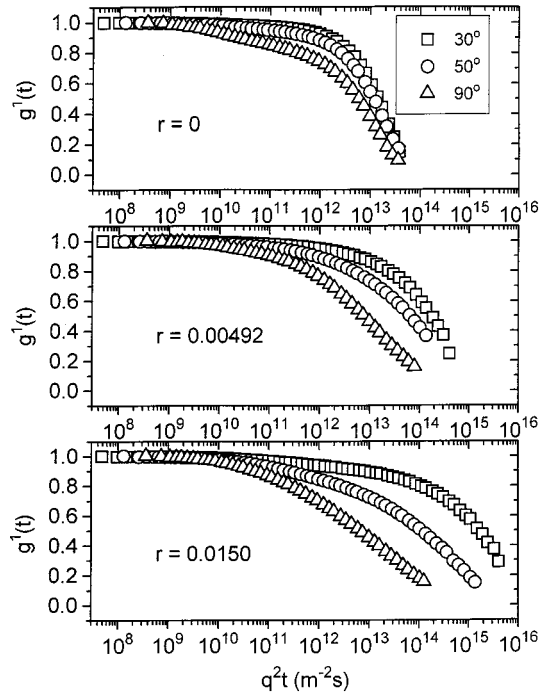

Figure 10. Plot of the first-order field correlation function versus q^2t (every third point is shown) for the mixture ratios (total polymer concentration of 1 wt %) and the scattering angles indicated.

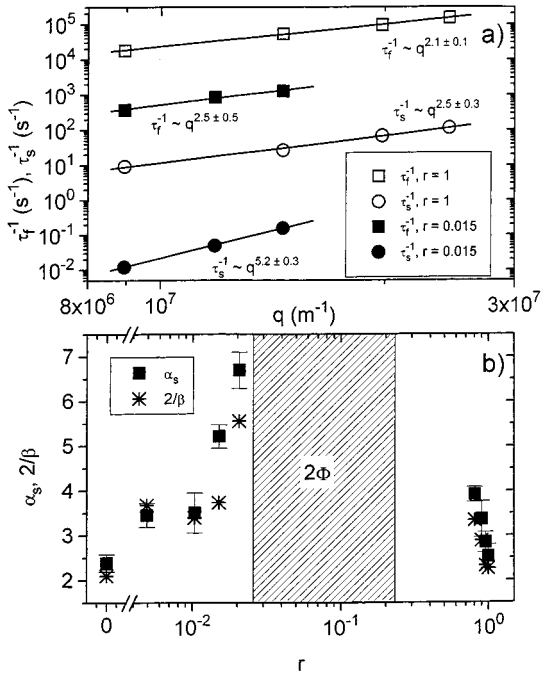

Figure 11. (a) Illustration of the wave vector dependences of the fast (τ_f^{-1}) and the slow (τ_s^{-1}) inverse relaxation times for the mixture ratios (total polymer concentration of 1 wt %) indicated. (b) Effects of the mixture ratio on the quantities $2/\beta$ (see the main text for explanation) and α_s, illustrating the q dependence of the slow inverse relaxation time.

If we follow the coupling approach, with $\phi(t)$ given by eqs 4 and 5, τ_0 of eq 4 arises from a purely diffusive process leading to a simple exponential decay, so its q dependence is given by

$$\tau_0(q) \sim q^{-2} \tag{7}$$

We may note that the q dependence of the fast mode in this work is consistent with this prediction. Substituting this expression for $\tau_0(q)$ into eq 6, a stronger q dependence of τ^*_s

$$\tau^*_s(q) = [t_c^{-n}\tau_0(q)]^{1/(1-n)} \sim q^{-2/(1-n)} \sim q^{-2/\beta} \tag{8}$$

is found. As the interaction is enhanced, there is a concomitant increase in the coupling parameter n, or a decrease of β, and the q dependence of τ_s becomes even stronger. A comparison between the experimental results and the values predicted with the aid of eq 8 is depicted in Figure 11b. The agreement between the experimental and the calculated values is reasonably good. As far as we know, this result is not predicted by any other model.

Intensity Light Scattering. An intensity light scattering experiment probes density correlations on a length scale q^{-1}. The properties of the light scattered by polymer solutions depend on the concentration range and on the relative magnitude of a characteristic length scale explored in the light scattering experiment. In semidilute solutions (as in the present work), i.e., above the overlap concentration, the characteristic length is the correlation length, which is on the order of the mesh size ξ of the network. This length characterizes the crossover between a "fractal" and a "homogeneous" structure.

In the Guinier region ($q\xi < 1$), the angular distribution of scattered intensity is observed, and the normalized inverse scattered intensity function can be described by a Ornstein−Zernike law[35]

$$S(0)/S(q) = 1 + q^2\xi^2 \tag{9}$$

where $S(q) = R_{vv}(q)/KcM$ and $S(0) = RT/M(\partial\Pi/\partial c)$, with R the gas constant, T the temperature, and $\partial\Pi/\partial c$ the inverse osmotic compressibility. From this relation, the static screening length is easily extractable. The results presented and discussed above showed (see Figure 7) that ξ increases as the two-phase region is approached. This indicates that the material is undergoing structural reorganization. The picture that emerges is that the singly stranded structure prevailing at conditions far away from the two-phase domain is replaced, at least in part, by denser bundles of chains, with a larger spacing between bundles (cf. Figure 8).

The angular dependence of the reciprocal normalized scattering intensity for systems of various mixture ratios is depicted in Figure 12. The results show that for solutions of the pure components there is a strong angular dependence, suggesting the existence of large entities, while for mixtures with compositions that are close to the two-phase region, there is virtually no q dependence. These findings may be interpreted in the following way. For a solution with a composition that is remote from the two-phase region, the conjecture is that the solution is composed of clusters that are imbricated, but they are not entangled as suggested by the liquidlike response from the rheological measurements. For mixtures close to the two-phase region, a strong interconnected network is established, and the angular dependence of the scattering intensity disappears. In this context we should note a previous light scattering study[26] on an aqueous thermoreversible system of ethyl(hydroxyethyl)cellulose in the presence of an ionic surfactant, where the angular dependence of the normalized inverse scattered intensity function was found to decline as the gel zone was approached.

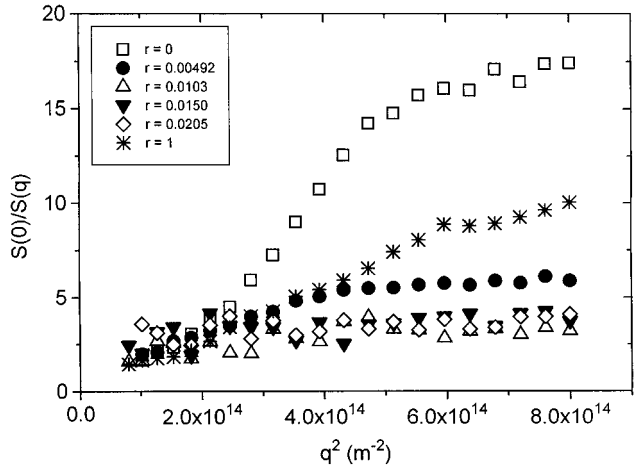

Figure 12. q^2 dependence of the reduced inverse scattered intensity function for the mixture ratios indicated (the total polymer concentration is 1 wt %).

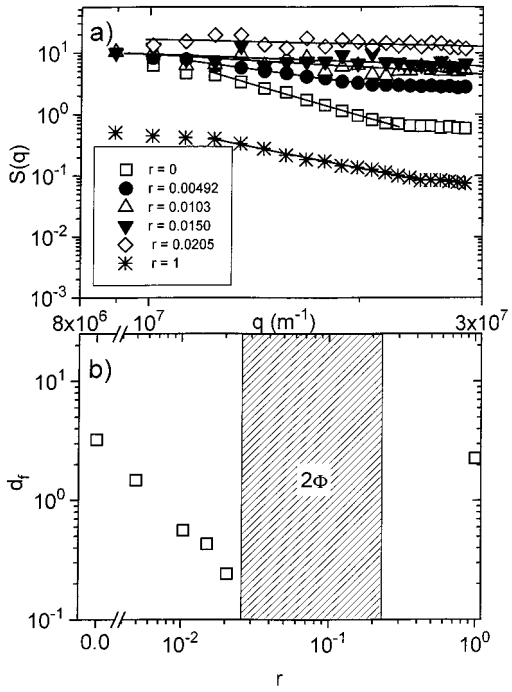

Figure 13. (a) A log−log plot of the q dependence of the scattered intensity function for the mixture ratios indicated (the total polymer concentration is 1 wt %). (b) The effect of mixture composition on the fractal dimension d_f (see eq 10).

This feature indicates that the network connectivity has a significant impact on the scattering pattern.

In the regime $q\xi > 1$, the length scale q^{-1} is associated with more local properties of the system, and the scattered intensity depends strongly on the length scale. We can view the semidilute solution as an irregular fractal network,[42] formed by more or less interpenetrating clusters. In this case the scattering intensity or the structure factor decays with the wave vector as

$$S(q) \sim q^{-d_f} \tag{10}$$

where the slope of the structure factor in the power-law regime yields the fractal dimension d_f ($0 < d_f \leq 3$).

Figure 13a shows the intensity profiles in form of log−log plots of $S(q)$ versus q for solutions of different ratios of mixture at a total polymer concentration of 1 wt %. The solid lines represent the best fit of the experimental data with eq 10 in the intermediate q regime. The fractal dimension of the clusters in solutions of the pure polyelectrolyte components is close to 3 (see Figure 13b), indicating a homogeneous structure. It is obvious that the value of d_f falls off strongly as the two-phase region is approached. These results suggest that the network structure becomes more "open"[43] in the vicinity of phase separation. This behavior is compatible with the hypothesis that an inhomogeneous network, containing bundles, is formed.

Conclusions

The results reported in this study emphasize the profound impact of the mixture ratio of oppositely charged and hydrophobically modified polyelectrolytes on the rheological, dynamical, and structural properties of these systems. The experiments have been carried out on aqueous solutions of pure polyelectrolytes and various mixtures. Mixtures of two oppositely charged and hydrophobically modified polyelectrolytes will have an inclination to associative phase separation, and due to the presence of hydrophobic tails, the system promotes the formation of mixed aggregates. This process is reminiscent of the phenomenon observed in systems of one ionic surfactant and one hydrophobically modified polymer. In the vicinity of the two-phase region, the charges on HM-P^+ are screened by those of the anionic polymer, and as a result, the hydrophobic interactions will grow in importance.

The rheological measurements reveal liquidlike response in solutions of the pure polyelectrolytes, while in mixtures of the two polyelectrolytes the elastic response becomes gradually more dominant as the two-phase region is approached. At this stage, the frequency dependences of the dynamic moduli cannot be described by a simple Maxwell model, but the rheological behavior is complex with a broad distribution of relaxation times. The rheological results favor the hypothesis of enhanced interactions when the two-phase region is approached.

The results from the DLS experiments indicate the existence of two relaxation modes, where the initial decay of the correlation function is described by a single exponential followed by a stretched exponential at longer times. The fast mode, which is always q^2 dependent, yields the cooperative diffusion coefficient and the hydrodynamic correlation length. Both the static and the hydrodynamic correlation lengths increase as the two-phase region is approached. The marked rise of the slow relaxation time, characterizing cluster disengagement relaxation, as well as the pronounced increase in the time of intersection from the rheological measurements suggests that strong associations are formed at mixture compositions toward phase separation. The q dependence of the slow mode is stronger than that of a diffusive process, and it increases steadily as the two-phase domain is approached. This feature, as well as the accompanying drop of the stretched exponential β, can be rationalized as enhanced intermolecular interactions within the framework of the coupling model of Ngai.

The intensity light scattering measurements revealed in the regime $q\xi > 1$ a power law in the form $S(q) \sim q^{-d_f}$, with a fractal dimension that falls off significantly in the direction of phase separation of the mixture. The overall picture that emerges from this study is that the polymer network undergoes a structural reorganization from a homogeneous singly stranded structure in the

solutions of the pure polyelectrolytes to an inhomogeneous network containing bundles of polycation and polyanion chains as the two-phase region is approached. As a result of this process, the average mesh size of the network increases significantly.

Acknowledgment. We are grateful to Dr. I. Iliopoulos for the kind supply of the hydrophobically modified polyacrylate. The Nils and Dorthi Troëdsson research foundation is acknowledged for a grant for the Carri-Med rheometer. M.T. and K.T. thank the NUTEK- and Industry Sponsored Centre for Amphiphilic Polymers (CAP) for financial support.

References and Notes

(1) Goddard, E. D. *Colloids Surf.* **1986**, *19*, 301.
(2) Piculell, L.; Lindman, B. *Adv. Colloid. Interface Sci.* **1992**, *41*, 149.
(3) Magny, B.; Iliopoulos, I.; Zana, R.; Audebert, R. *Langmuir* **1994**, *10*, 3180.
(4) Guillemet, F.; Piculell, L. *J. Phys. Chem.* **1995**, *99*, 9201.
(5) Okuzaki, H.; Osada, Y. *Macromolecules* **1995**, *28*, 4554.
(6) Guillemet, F.; Piculell, L.; Nilsson, S.; Djabourov, M.; Lindman, B. *Prog. Colloid Polym. Sci.* **1995**, *98*, 47.
(7) Wallin, T.; Linse, P. *Langmuir* **1998**, *14*, 2940.
(8) Thalberg, K.; Lindman, B. *Interactions of Surfactants with Polymers and Proteins*; Goddard, E. D., Ananthapadmanabhan, K. P., Eds.; CRC Press: Boca Raton, FL, 1993; pp 203−276.
(9) Michaels, A. S.; Miekka, R. G. *J. Phys. Chem.* **1961**, *65*, 1765.
(10) Tsuchida, E.; Osada, Y.; Sanada, K. *J. Polym. Sci. A-1* **1972**, *10*, 3397.
(11) Abe, K.; Koide, M.; Tsuchida, E. *J. Polym. Sci., Polym. Chem. Ed.* **1977**, *15*, 2469.
(12) Kabanov, V. A.; Zezin, A. B. *Sov. Sci. Rev., Ser. B* **1982**, *4*, 207.
(13) Senuma, M.; Kuwabara, S.; Kaeriyama, K.; Shimura, Y. *J. Appl. Polym. Sci.* **1986**, *31*, 1687.
(14) Burkart, P.; Dautzenberg, H.; Linow, K.-J.; Kötz, J.; Dawydoff, W. *Prog. Polym. Sci.* **1989**, *14*, 91.
(15) Frugier, D.; Audebert, R. In *Macromolecular Complexes in Chemistry and Biology*; Dubin, P., Bock, J., Davies, R. M., Schulz, D. N., Thies, C., Eds.; Springer-Verlag: Berlin, 1994; p 134.
(16) Nyrkova, I. A.; Khokhlov, A. R.; Doi, M. *Macromolecules* **1994**, *27*, 4220.
(17) Thuresson, K.; Nilsson, S.; Lindman, B. *Langmuir* **1996**, *12*, 530.
(18) Pogodina, N. V.; Tsvetkov, N. V. *Macromolecules* **1997**, *30*, 4897.
(19) Zezin, A. B.; Rogacheva, V. B.; Kabanov, V. A. *Macromol. Symp.* **1997**, *126*, 123.
(20) Dhoot, S.; Goddard, E. D.; Murphy, D. S.; Tirrell, M. *Colloids Surf.* **1992**, *66*, 91.
(21) Wang, K. T.; Iliopoulos, I.; Audebert, R. *Polym. Bull.* **1988,** *20*, 577.
(22) Chu, B.; Onclin, M.; Ford, J. R. *J. Phys. Chem.* **1984**, *88*, 6566.
(23) Guinier, A.; Fournet, G. *Small Angle Scattering of X-rays;* J. Wiley & Sons: New York, 1955.
(24) Siegert, A J. F. Massachusetts Institute of Technology Rad. Lab. Rep. No. 456, 1943.
(25) Martin, J. E.; Wilcoxon, J.; Odinek, J. *Phys. Rev. A* **1991**, *43*, 858.
(26) Nyström, B.; Roots, J.; Carlsson, A.; Lindman, B. *Polymer* **1992**, *33*, 2875.
(27) Wang, C. H.; Zhang, X. Q. *Macromolecules* **1993**, *26*, 707.
(28) Nyström, B.; Walderhaug, H.; Hansen, F. K. *J. Phys. Chem.* **1993**, *97*, 7743.
(29) Raspaud, E.; Lairez, D.; Adam, M.; Carton, J.-P. *Macromolecules* **1994**, *27*, 2956.
(30) Nyström, B.; Lindman, B. *Macromolecules* **1995**, *28*, 967.
(31) Nyström, B.; Thuresson, K.; Lindman, B. *Langmuir* **1995**, *11*, 1994.
(32) Douglas, J. F.; Hubbard, J. B. *Macromolecules* **1991**, *24*, 3163.
(33) Ngai, K. L. *Adv. Colloid Interface Sci.* **1996**, *64*, 1.
(34) Thuresson, K.; Lindman, B.; Nyström, B. *J. Phys. Chem. B* **1997**, *101*, 6450.
(35) De Gennes, P.-G. *Scaling Concepts in Polymer Physics*; Cornell University Press: Ithaca, NY, 1979.
(36) Hecht, A.-M-; Guillermo, A.; Horkay, F.; Mallam, S.; Legrand, J. F.; Geissler, E. *Macromolecules* **1992**, *25*, 3677.
(37) Rendell, R. W.; Ngai, K. L.; McKenna, G. B. *Macromolecules* **1987**, *20*, 2250.
(38) Ngai, K. L.; Peng, S. L.; Tsang, K. Y. *Physica A* **1992**, *191*, 523.
(39) Ngai, K. L. In *Disorder Effects in Relaxation Processes*; Richert, R., Blumen, A., Eds.; Springer-Verlag: Berlin, 1994; p 89.
(40) Tsang, K. Y.; Ngai, K. L. *Phys. Rev. E* **1996**, *54*, R3067.
(41) Ngai, K. L.; Phillies, G. D. J. *J. Chem. Phys.* **1996**, *105*, 8385.
(42) Daoud, M.; Leibler, L. *Macromolecules* **1988**, *21*, 1497.
(43) Muthukumar, M. *Macromolecules* **1989**, *22*, 4656.

MA981619C